DOI: 10.1002/chem.201002292

Preparation of Surface Organometallic Catalysts by Gas-Phase Ligand Stripping and Reactive Landing of Mass-Selected Ions

Grant E. Johnson and Julia Laskin*[a]

Abstract: Organometallic complexes immobilized on surfaces combine the high selectivity of homogeneous catalysts with the ease of separation of catalyst from products attainable with heterogeneous catalysts. Here we report a novel approach for the highly controlled preparation of surface organometallic catalysts by gas-phase ligand stripping combined with reactive landing of mass-selected ions onto self-assembled monolayer surfaces. Collision-induced dissociation is used to generate highly reactive undercoordinated metal complexes in the gas-phase for subsequent surface immobilization. Complexes with an open coordination shell around the metal center are demonstrated to show enhanced activity towards reactive landing in comparison to fully ligated species. In situ TOF-SIMS analysis indicates that the immobilized complexes exhibit behavior consistent with catalytic activity when exposed to gaseous reagents.

Keywords: collision induced dissociation · heterogeneous catalysis · mass spectrometry · organometallic complex · reactive landing

Introduction

Solution-phase organometallic complexes are employed as catalysts to promote a variety of commercially important reactions.[1–2] Homogeneous catalysts exhibit extremely high selectivity towards desired products due to the well-defined, single-site nature of the active species.[3] In contrast, solid-phase heterogeneous catalysts often contain a distribution of different surface sites which results in relatively higher yields of unwanted byproducts.[4] While this lack of selectivity increases the energy demands and waste disposal associated with chemical production, heterogeneous catalysts find widespread application in industry due to the facile separation of products from remaining reactants and catalyst materials. Recently, efforts have been undertaken to combine the most beneficial aspects of homogeneous and heterogeneous catalysts by creating cooperative hybrid organic-inorganic interfaces.[5] Through immobilization of metal complexes on supports such as silica, surface organometallic catalysts have been generated and shown to exhibit activity towards industrially relevant reactions such as olefin polymerization and metathesis.[6] However, existing solution-phase techniques for producing these materials often require relatively large quantities of reactants and solvents and involve lengthy purification steps.[7]

Herein, we describe a novel approach for the highly controlled preparation of surface organometallic catalysts by gas-phase ligand stripping combined with reactive landing of mass-selected ions onto functionalized self assembled monolayers on gold (SAMs). Deposition of polyatomic ions onto surfaces is a promising approach for the preparation of materials[8–11] including model heterogeneous catalysts.[12–14] For instance, a recent study by Nakajima and co-workers demonstrated facile matrix isolation of vanadium–benzene sandwich clusters through ion soft landing.[15] In addition, a previous publication from our group describes an investigation of the charge retention and neutralization behavior of organometallic metal–salen complexes soft landed onto 1*H*,1*H*,2*H*,2*H*-perfluorododecane-1-thiol (FSAM) and 1-dodecanethiol self-assembled monolayer (HSAM) surfaces on gold.[16] More recently, in a collaborative study, we demonstrated that acid-mediated redox chemistry may be observed in thin films of organometallic complexes prepared by ion soft landing.[17] Mass selection enables species with well defined charge and chemical composition to be delivered to surfaces under controlled conditions. Consequently, further purification steps to remove unwanted contaminants, which are critical with solution-phase techniques, are avoided

---

[a] Dr. G. E. Johnson, Dr. J. Laskin
Chemical and Materials Sciences Division
Pacific Northwest National Laboratory, P.O. Box 999
MSIN K8-88, Richland, Washington 99352 (USA)
Fax: (+1) 509-371-6139
E-mail: grant.johnson@pnl.gov
julia.laskin@pnl.gov

using the ion landing approach. Mass spectrometry also provides a unique opportunity for the preparation of materials that are either inaccessible or extremely difficult to make in solution. Here, we show that gas-phase ligand stripping may be used to generate highly reactive undercoordinated metal complexes for subsequent immobilization on surfaces. Species with an open coordination shell around the metal center are demonstrated to exhibit enhanced activity towards reactive landing in comparison to those that are fully ligated. Moreover, the immobilized metal complexes are shown to exhibit behavior consistent with catalytic activity when exposed to gaseous reagents.

The ruthenium tris(bipyridine) [$Ru(bpy)_3$] complex has been a subject of recent interest due to its potential application as a photosensitizer in water oxidation catalysis.[18–19] Mixed ligand ruthenium complexes containing bipyridine have also been demonstrated to be effective catalysts for olefin expoxidation.[20] In addition, carbonyl containing ruthenium bis- and mono-bipyridine complexes have been shown to promote the water–gas shift reaction and reduction of CO_2.[21] In this study, we used the $Ru(bpy)_3^{2+}$ and $Ru(bpy)_2^{2+}$ dications to examine how a closed versus an open coordination shell around the ruthenium metal center impacts the efficiency of reactive landing of organometallic complexes and their subsequent activity towards gaseous reagents.

Results and Discussion

Reactive landing of mass selected ions: Figure 1a and b present the time of flight secondary ion mass spectrometry (TOF-SIMS) spectra (*m/z* 200–800) obtained after deposition of an equal quantity of $Ru(bpy)_3^{2+}$ and $Ru(bpy)_2^{2+}$ ions, respectively, onto two different COOH–SAM surfaces. As shown in Figure 1a, peak envelopes corresponding to $Ru(bpy)_3^{2+}$ *m/z* 285.06 and $Ru(bpy)_3^{+}$ *m/z* 570.1 are observed following deposition of fully ligated $Ru(bpy)_3^{2+}$ onto COOH–SAM surfaces. The relative abundances of these species indicate that partial charge reduction of $Ru(bpy)_3^{2+}$ to $Ru(bpy)_3^{+}$ occurs rapidly on the COOH–SAM, although charge exchange and loss processes are also possible during SIMS analysis. Another major peak envelope is observed in Figure 1a at *m/z* 414.05 and corresponds to $Ru(bpy)_2^{+}$. This species, which results from the loss of one bipyridine ligand from $Ru(bpy)_3^{+}$, is likely formed through fragmentation of $Ru(bpy)_3^{+}$ during SIMS analysis. In addition, a less abundant envelope of peaks is observed around *m/z* 562. This species also has been observed following deposition of $Ru(bpy)_3^{2+}$ onto FSAM as well as other SAM surfaces. While we do not have a definitive chemical assignment at this time, we propose that this peak envelope may correspond to $Ru(bpy)_2(C_{16}H_{12}O_4)^{+}$ which is produced from reaction of the deposited $Ru(bpy)_3^{2+}$ ion with residual organic impurities in the monolayer.[22] Indeed, recent studies have shown that the commercial methanol used to prepare the COOH–SAM monolayers contains organic impurities that can lead to the formation of larger hydrocarbon species.[23] Close inspection of Figure 1a also reveals a very low abundance peak envelope centered at *m/z* 700.2 which is consistent with doubly ligated $Ru(bpy)_2$ bound to an intact COOH terminated thiol ($C_{16}H_{30}O_2S$). Examination of the $Ru(bpy)_2(C_{16}H_{30}O_2S)^{+}$ peak envelope reveals that the isotopic pattern of the experimental TOF-SIMS spectrum matches, almost perfectly, the simulated pattern calculated using the molecular weight calculator program (http://omics.pnl.gov/software/MWCalculator.php) shown below in the inset of Figure 1b. Figure 1a, consequently, indicates that deposition of triply ligated ruthenium bipyridine ions onto COOH terminated SAMs results in the formation of a strong bond between a small portion of the deposited metal complexes and the terminal carboxylic acid group of the alkyl thiol. This is an intriguing observation as analyte–thiol peaks are not typically observed in TOF-SIMS spectra following soft landing without formation of a chemical bond. In previous studies of the deposition of peptides onto N-hydroxysuccinimidyl ester-terminated (NHS–SAM) surfaces, such thiol-adducts were only observed following reactive landing involving the formation of covalent bonds.[24] Carboxylic acid groups are known to interact with metals to form a salt and hydrogen. Such a reaction resulting in a surface bound $Ru(bpy)_2(C_{16}H_{30}O_2S)$ complex is consistent with the peaks observed at *m/z* 700.2.

The mass spectrum obtained following deposition of undercoordinated $Ru(bpy)_2^{2+}$ onto COOH–SAM is shown in Figure 1b. The $Ru(bpy)_2^{2+}$ ion is generated by the removal of one bipyridine ligand from $Ru(bpy)_3^{2+}$ through collision induced dissociation (CID) in the first collision quadrupole of the deposition instrument. The spectrum in Figure 1b lacks any of the features related to the fully ligated complex,

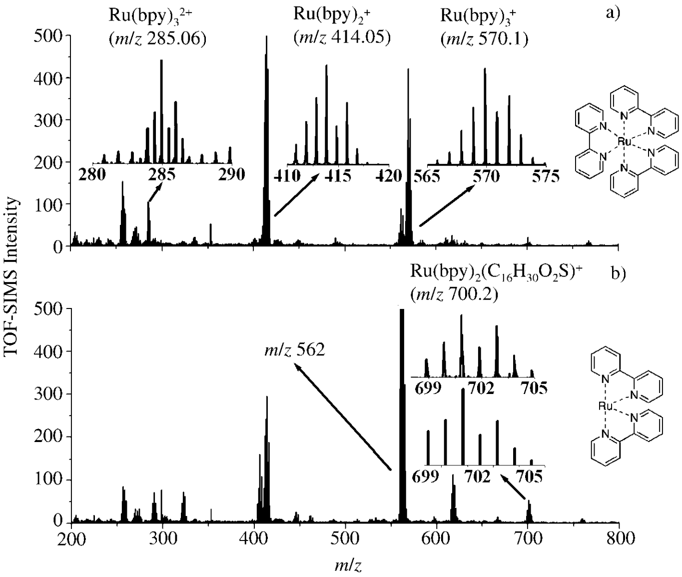

Figure 1. TOF-SIMS spectra (*m/z* 200–800) obtained after mass-selected deposition of a) $Ru(bpy)_3^{2+}$ and b) $Ru(bpy)_2^{2+}$ onto COOH–SAM. The inset spectrum shown below is the calculated isotope distribution of $Ru(bpy)_2(C_{16}H_{30}O_2S)^{+}$.

$Ru(bpy)_3^{2+}$ or $Ru(bpy)_3^+$. However, close inspection reveals the presence of several peaks in Figure 1 b that are not present in Figure 1 a. For example, new peak envelopes are observed around *m*/*z* 320 and 405, both of which have isotopic distributions consistent with species containing Ru. Furthermore, the $Ru(bpy)_2(C_{16}H_{12}O_4)^+$ impurity peak envelope centered around *m*/*z* 562 is far more abundant. This indicates that there are a few side products of reactive landing that are more abundant following deposition of $Ru(bpy)_2^{2+}$ compared to $Ru(bpy)_3^{2+}$. Of particular interest to this study, however, is the $Ru(bpy)_2(C_{16}H_{30}O_2S)$ peak envelope centered at *m*/*z* 700.2 which exhibits greatly enhanced abundance in Figure 1 b compared to Figure 1 a. The two spectra, consequently, indicate that deposition of both triply and doubly ligated ruthenium–bipyridine ions onto COOH terminated SAMs results in the formation of the immobilized $Ru(bpy)_2(C_{16}H_{30}O_2S)$ complex. Moreover, a significantly higher yield of this complex is obtained if one of the bipyridine ligands is removed in the gas-phase prior to deposition.

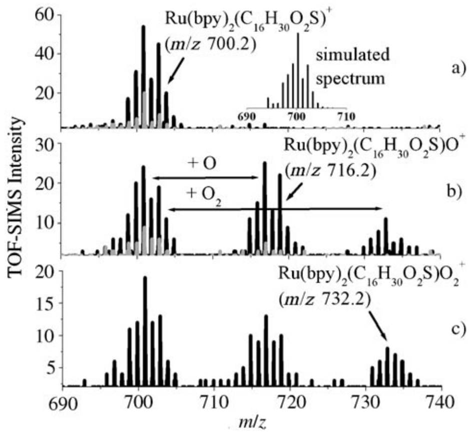

Figure 2. TOF-SIMS spectra (*m*/*z* 690–740) obtained a) after mass-selected deposition of $Ru(bpy)_2^{2+}$ (black) and $Ru(bpy)_3^{2+}$ (grey) onto COOH–SAM, b) after exposure to O_2 and c) after exposure to C_2H_4.

Figure 2 a presents the mass spectra, overlaid and focused on the region of interest at *m*/*z* 690–740. The spectra obtained following deposition of $Ru(bpy)_3^{2+}$ and $Ru(bpy)_2^{2+}$ are shown in grey and black, respectively. Again, comparison of the relative abundances of the peaks in Figure 2 a emphasizes that a much higher yield of the thiol-bound Ru complex is obtained when one of the bipyridine ligands is removed in the gas phase prior to deposition. As shown in Scheme 1, therefore, gas-phase ligand stripping may be used to generate undercoordinated metal complexes which exhibit enhanced activity towards reactive landing on functionalized monolayers in comparison to fully ligated metal centers. The fact that a smaller yield of the immobilized complex is observed following deposition of the fully ligated ion suggests that only a fraction of the $Ru(bpy)_3^{2+}$ ions have sufficient energy to undergo reaction. The reaction of the fully ligated complex with the COOH–SAM surface most likely involves stripping of one bipyridine ligand at the time of collision with the surface followed by covalent immobilization of the resulting undercoordinated species.

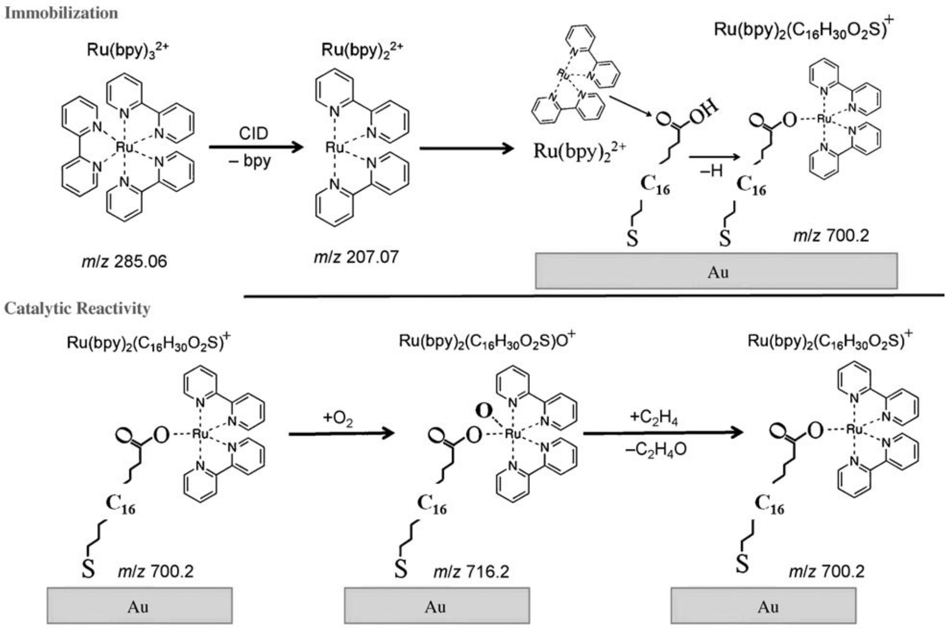

Scheme 1. Graphical representation of the immobilization of $Ru(bpy)_3^{2+}$ on COOH–SAM surfaces through gas-phase ligand stripping and reactive landing of mass-selected ions.

Reactive gas exposure: To examine the reactivity of the immobilized organometallic complexes the SAM surfaces were exposed sequentially to O_2 followed by C_2H_4 and analyzed by in situ TOF-SIMS. The spectra obtained following exposure sequentially to O_2 followed by C_2H_4 are presented in Figure 2 b and c, respectively. As shown in Figure 2 a, immediately following deposition of $Ru(bpy)_2^{2+}$ onto COOH–SAM, only the isotopic envelope of the immobilized complex, $Ru(bpy)_2(C_{16}H_{30}O_2S)^+$, is observed in the mass range of *m*/*z* 690–740. However, after exposure to O_2 for 30 min, there is a pronounced decrease in the relative abundance of $Ru(bpy)_2(C_{16}H_{30}O_2S)^+$ at *m*/*z* 700.2 and a concomitant increase in the abundance of peak envelopes centered at *m*/*z* 716.2 and 732.2 corresponding to addition of O and O_2, respectively, to the immobilized complex. The secondary ion yields of these complexes are all expected to be very similar. The spectra suggest that the immobilized $Ru(bpy)_2(C_{16}H_{30}O_2S)^+$ complex is reactive towards O_2 and generates the oxidized complexes $Ru(bpy)_2(C_{16}H_{30}O_2S)O^+$ and $Ru(bpy)_2(C_{16}H_{30}O_2S)O_2^+$ with approximately 50% conversion efficiency. We are confident that these oxidized species result from interaction of the immobilized $Ru(bpy)_2(C_{16}H_{30}O_2S)$ complex with O_2 and not from oxidation of the alkyl thiol because the substrates are exposed to an oxidizing air environment during preparation and no oxygen adducts are observed in the SIMS spectrum acquired prior to ion deposition. Such species are only present following reactive landing of $Ru(bpy)_{2-3}{}^{2+}$ and exposure to O_2.

Following in situ analysis of the oxidized substrate, the surface was transferred back into the deposition instrument and exposed to C_2H_4. After 30 min of C_2H_4 exposure the substrate was moved back into the UHV SIMS chamber and reanalyzed. The TOF-SIMS spectrum obtained following exposure to C_2H_4 is presented in Figure 2c. The spectrum indicates a preferential decrease in the relative abundance of the oxidized complex $Ru(bpy)_2(C_{16}H_{30}O_2S)O^+$ at *m/z* 716.2. There is also a minor decrease in the overall abundances of the peaks corresponding to $Ru(bpy)_2(C_{16}H_{30}O_2S)^+$ *m/z* 700.2 and $Ru(bpy)_2(C_{16}H_{30}O_2S)O_2^+$ *m/z* 732.2. The depletion of these species is likely due to association of C_2H_4 related cracking products onto the immobilized organometallic complexes which results in their conversion to higher *m/z* adducts as discussed below. Nevertheless, comparison of the spectra in Figure 2b and c indicates that exposure to ethylene results in preferential depletion of $Ru(bpy)_2(C_{16}H_{30}O_2S)O^+$, consistent with deoxygenation of the immobilized organometallic complex. Close inspection of Figure 2c also reveals that the envelope of peaks corresponding to the oxidized complex centered at *m/z* 716.2 changes somewhat following exposure to C_2H_4. In particular, the peaks at *m/z* 714.2 and 715.2 appear relatively more abundant in relation to the primary peak at *m/z* 716.2. In addition to deoxygenation, therefore, upon exposure to C_2H_4 there appears to be association of CH_2 (+14) or CH_3 (+15) onto $Ru(bpy)_2(C_{16}H_{30}O_2S)$ *m/z* 700.2 forming $Ru(bpy)_2(C_{16}H_{30}O_2S)CH_2$ *m/z* 714.2 and $Ru(bpy)_2(C_{16}H_{30}O_2S)CH_3$ *m/z* 715.2. As shown in Scheme 1, therefore, the immobilized complex exhibits behavior consistent with hydrocarbon oxidation and cracking reactions, both of which are of significant importance to commercial chemical production.[25]

After completion of the first oxidation and reduction cycle, the surface was exposed sequentially to O_2 followed by C_2H_4 for a second time. The ratios of the integrated abundances of the primary isotope for $Ru(bpy)_2(C_{16}H_{30}O_2S)^+$ and $Ru(bpy)_2(C_{16}H_{30}O_2S)O^+$ after exposure to O_2 followed by C_2H_4 serve as an indicator of the degree of oxidation or reduction of the immobilized complex and are presented in Figure 3. The abundance ratios of the primary isotopes were plotted rather than the summed abundances of the entire peak envelopes to avoid errors in the ratios that would result from the CH_2 and CH_3 association products discussed previously. There are four data points presented in Figure 3, each taken after a separate reactive gas exposure. The line connecting the points serves to guide the eye. Despite the decrease in overall abundance with repeated gas exposures the ratios display a clear cyclical oscillatory behavior depending on whether the surface has been exposed to O_2 or C_2H_4 prior to analysis by in situ TOF-SIMS. The ratios indicate that there is an increase in the relative abundance of $Ru(bpy)_2(C_{16}H_{30}O_2S)O^+$ following exposure of the surface to oxygen and an increase in the abundance of $Ru(bpy)_2(C_{16}H_{30}O_2S)^+$ following exposure to C_2H_4. Moreover, this oxidation–reduction cycle may be repeated multiple times consistent with catalytic behavior. In comparison, soft landed $Ru(bpy)_3{}^{2+}$ does not show this behavior indicating that through gas-phase ligand stripping it is possible to convert a relatively inert fully ligated complex into a catalytically active undercoordinated species that is easy to immobilize on SAM surfaces through reactive landing. Repeat experiments performed on different days reveal that while the overall abundance of ions observed in the TOF-SIMS spectra may vary somewhat depending on the quality of the COOH–SAM surface, the tuning of the deposition and SIMS analysis instruments, and the quantity of deposited ions, the relative abundances of surface peaks with respect to each other consistently exhibit the oscillatory behavior shown in Figure 3 following exposure to O_2 or C_2H_4. Therefore, while quantitative statistics were not obtained the data are qualitatively consistent from experiment to experiment.

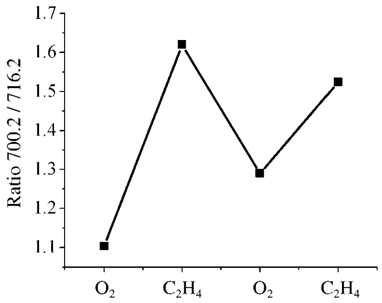

Figure 3. Ratio of the TOF-SIMS abundances of $Ru(bpy)_2(C_{16}H_{30}O_2S)^+$ (*m/z* 700.2) to $Ru(bpy)_2(C_{16}H_{30}O_2S)O^+$ (*m/z* 716.2) obtained after exposure to O_2 and C_2H_4.

Conclusion

In summary, this study demonstrates for the first time that gas-phase ligand stripping combined with reactive landing of mass-selected ions may be used to prepare surface organometallic catalysts that are not easily accessible using conventional techniques. Surface characterization by in situ TOF-SIMS indicates that by removing a ligand in the gas-phase by CID it is possible to promote the reactive landing of metal complexes that are otherwise largely unreactive when soft landed. Moreover, the in situ SIMS technique allows the reactivity of the immobilized complexes towards gaseous reagents to be studied providing evidence of catalytic behavior.

Experimental Section

Reactive landing of mass selected ions: The results described herein were obtained using a recently constructed ion deposition instrument coupled to a time-of-flight secondary ion mass spectrometer (TOF-SIMS) described elsewhere.[22] Briefly, doubly charged $Ru(bpy)_3^{2+}$ ions were generated through electrospray ionization, introduced into vacuum using an electrodynamic ion funnel, focused in a collision quadrupole, mass selected with a quadrupole mass filter, deflected 90° by a quadrupole bender, and transferred to the surface through a series of two Einzel lenses. The doubly charged $Ru(bpy)_3^{2+}$ ion results from dissolution and dissociation of tris(2,2′-bipyridyl)dichlororuthenium(II) hexahydrate in methanol solution and was mass-selected for deposition because it is the dominant ion generated by electrospray ionization. Undercoordinated $Ru(bpy)_2^{2+}$ ions were generated by removal of one bipyridine ligand from fully ligated $Ru(bpy)_3^{2+}$ through gas-phase collision induced dissociation (CID) in the first collision quadrupole of the deposition instrument. An optimized ion current of 65 and 45 pA was directed at the surface for 90 and 120 min for $Ru(bpy)_3^{2+}$ and $Ru(bpy)_2^{2+}$, respectively, corresponding to a total delivery of 1.1×10^{12} ions to a circular spot 3 mm in diameter. The kinetic energy of the ions impacting the surface was controlled by adjusting the potentials applied to the second collision quadrupole and the surface and was set at 25 eV per charge for all of the experiments described herein. Assuming that all of the ions retain their charge once deposited onto the surface, the maximum potential resulting from the total charge delivered by the ion beam to the surface can be estimated[26] and was calculated to be 2.5 V for 10^{12} doubly charged $Ru(bpy)_{2-3}^{2+}$ ions delivered to a spot size of 3 mm. Because this potential is much smaller than the kinetic energy of the ions, it does not interfere with ion deposition. It follows that all of the ions delivered to the substrate are able to approach the surface and can become immobilized.

In situ TOF-SIMS analysis: In situ analysis of surfaces was performed using 15 keV Ga^+ TOF-SIMS in a commercial PHI TRIFT II instrument (Physical Electronics, Eden Prairie, MN). In TOF-SIMS the sample is bombarded by 15 keV primary gallium ions (Ga^+, 500 pA, 5 ns pulse width, 10 kHz repetition rate) which induces desorption of material from the surface. The secondary ions ejected from the surface are extracted into the mass analyzer which consists of three separate electrostatic sectors. The mass spectrometer compensates for any energy dispersion of the secondary ions and achieves a mass resolution of around 4000 at 1000 amu. All spectra were acquired for 2 min.

Reactive gas exposure: Following reactive landing the substrates were sequentially exposed in the deposition instrument to controlled pressures of 1×10^{-4} Torr of oxygen (O_2) followed by ethylene (C_2H_4) for 30 min per exposure. After each gas exposure the surface was transferred into the analysis chamber (~10^{-9} Torr) and analyzed by in situ TOF-SIMS. To ensure that each SIMS spectrum was obtained at the center of the spot of deposited ions TOF-SIMS line profiles were obtained along both the x and y axis of the substrate. The line profiles for $Ru(bpy)_{2-3}$ related peaks (data not shown) reveal a Gaussian-like distribution of ion abundances with a spot diameter of approximately 3 mm in both dimensions. While the overall abundance of deposited ions exhibits a Gaussian like distribution across the deposited spot, the relative abundances of different ions with respect to each other is observed to be fairly constant across the spot profile. All of the mass spectra presented in this work were obtained at the center of the spot where the ion abundances were highest.

Materials: The gold substrates used to create alkyl thiol self-assembled monolayers were purchased from Platypus Technologies (Madison, WI) and have the following specifications: 10×10 mm, 525 um thick Si, 50 Å Ti adhesion layer, 1000 Å Au layer. 16-Mercaptohexadecanoic acid was purchased from Asemblon (Asemblon Inc., Redmond, WA). The COOH–SAM surfaces were prepared following literature procedures[27] with the substitution of HPLC grade methanol as the solvent which was purchased from Fisher (Fisher Scientific, Pittsburgh, PA). The acetic acid used for the preparation of the COOH–SAM was also purchased from Fisher. The gold substrates were cleaned using a Boekel (Boekel Scientific, Feasterville, PA) ultraviolet cleaner and immersed in glass scintillation vials containing 1 mM solutions of thiol in a methanol/acetic acid solvent. The monolayers were allowed to assemble for at least 12 h and then ultrasonically washed for 5 min in a methanol acetic acid solution. The surfaces were then rinsed with pure methanol, dried with N_2 and mounted in the SIMS sample holder. A background TOF-SIMS spectrum was obtained for each COOH–SAM surface prior to ion deposition to ensure that a clean well assembled monolayer was formed. Tris(2,2′-bipyridyl)dichlororuthenium(II) hexahydrate was purchased from Sigma–Aldrich. The powder was dissolved in methanol to create stock solutions with a concentration of 1×10^{-3} M. The stock solutions were diluted by either a factor of 10 or 100 to achieve optimum electrospray ion signal.

Acknowledgements

The authors acknowledge support for this research by a grant from the Chemical Sciences Division, Office of Basic Energy Sciences of the U.S. Department of Energy (DOE), and the Laboratory Directed Research and Development Program at the Pacific Northwest National Laboratory (PNNL). This work was performed at the W. R. Wiley Environmental Molecular Sciences Laboratory (EMSL), a national scientific user facility sponsored by the U.S. DOE of Biological and Environmental Research and located at PNNL. PNNL is operated by Battelle for the U.S. DOE.

---

[1] W. A. Herrmann, B. Cornils, *Angew. Chem.* **1997**, *119*, 1074–1095; *Angew. Chem. Int. Ed.* **1997**, *36*, 1049–1067.
[2] G. W. Parshall, *J. Mol. Catal.* **1978**, *4*, 243–270.
[3] R. T. Baker, S. Kobayashi, W. Leitner, *Adv. Synth. Catal.* **2006**, *348*, 1337–1340.
[4] G. A. Somorjai, C. J. Kliewer, *React. Kinet. Catal. Lett.* **2009**, *96*, 191–208.
[5] J. M. Notestein, A. Katz, *Chem. Eur. J.* **2006**, *12*, 3954–3965.
[6] C. Copéret, *New J. Chem.* **2004**, *28*, 1–10.
[7] M. Chabanas, A. Baudouin, C. Coperet, J. M. Basset, *J. Am. Chem. Soc.* **2001**, *123*, 2062–2063.
[8] S. A. Miller, H. Luo, S. J. Pachuta, R. G. Cooks, *Science* **1997**, *275*, 1447–1450.
[9] Z. Ouyang, Z. Takats, T. A. Blake, B. Gologan, A. J. Guymon, J. M. Wiseman, J. C. Oliver, V. J. Davisson, R. G. Cooks, *Science* **2003**, *301*, 1351–1354.
[10] B. Gologan, J. R. Green, J. Alvarez, J. Laskin, R. G. Cooks, *Phys. Chem. Chem. Phys.* **2005**, *7*, 1490–1500.
[11] D. Löffler, N. Bajales, M. Cudaj, P. Weis, S. Lebedkin, A. Bihlmeier, D. P. Tew, W. Klopper, A. Bottcher, M. M. Kappes, *J. Chem. Phys.* **2009**, *130*, -.
[12] S. Vajda, R. E. Winans, J. W. Elam, B. D. Lee, M. J. Pellin, S. Seifert, G. Y. Tikhonov, N. A. Tomczyk, *Top Catal.* **2006**, *39*, 161–166.
[13] U. Heiz, E. L. Bullock, *J. Mater. Chem.* **2004**, *14*, 564–577.
[14] W. P. Peng, M. P. Goodwin, Z. X. Nie, M. Volny, O. Y. Zheng, R. G. Cooks, *Anal. Chem.* **2008**, *80*, 6640–6649.
[15] M. Mitsui, S. Nagaoka, T. Matsumoto, A. Nakajima, *J. Phys. Chem. B* **2006**, *110*, 2968–2971.
[16] J. Laskin, P. Wang, O. Hadjar, *J. Phys. Chem. C* **2010**, *114*, 5305–5311.
[17] W. P. Peng, G. E. Johnson, I. Fortmeyer, P. Wang, O. Hadjar, R. G. Cooks, J. Laskin, *Phys. Chem. Chem. Phys.* **2010** DOI: 10.1039/c0cp01457e.
[18] J. J. Concepcion, J. W. Jurss, M. K. Brennaman, P. G. Hoertz, A. O. T. Patrocinio, N. Y. M. Iha, J. L. Templeton, T. J. Meyer, *Acc. Chem. Res.* **2009**, *42*, 1954–1965.
[19] X. Sala, I. Romero, M. Rodriguez, L. Escriche, A. Llobet, *Angew. Chem.* **2009**, *121*, 2882–2893; *Angew. Chem. Int. Ed.* **2009**, *48*, 2842–2852.
[20] M. J. Upadhyay, P. K. Bhattacharya, P. A. Ganeshpure, S. Satish, *J. Mol. Catal.* **1993**, *80*, 1–9.
[21] M. Haukka, P. Hirva, S. Luukkanen, M. Kallinen, M. Ahlgren, T. A. Pakkanen, *Inorg. Chem.* **1999**, *38*, 3182–3189.

[22] G. E. Johnson, M. Lysonski, J. Laskin, *Anal. Chem.* **2010**, *82*, 5718–5727.
[23] G. Guella, D. Ascenzi, P. Franceschi, P. Tosi, *Rapid Commun. Mass Spectrom.* **2007**, *21*, 3337–3344.
[24] P. Wang, O. Hadjar, P. L. Gassman, J. Laskin, *Phys. Chem. Chem. Phys.* **2008**, *10*, 1512–1522.
[25] G. A. Somorjai, J. Y. Park, *Chem. Soc. Rev.* **2008**, *37*, 2155–2162.
[26] J. Laskin, P. Wang, O. Hadjar, *Phys. Chem. Chem. Phys.* **2008**, *10*, 1079–1090.
[27] H. Wang, S. F. Chen, L. Y. Li, S. Y. Jiang, *Langmuir* **2005**, *21*, 2633–2636.

Received: August 11, 2010